

Supplementary Information for

Mapping Polysulfides in Sodium-Sulfur Batteries

Esther Lilian Gray¹, Jung-In Lee¹, Zhuangnan Li¹, James Moloney¹, Ziwei Jeffrey Yang¹,

Manish Chhowalla^{1}*

¹Department of Materials Science and Metallurgy, University of Cambridge, Cambridge,

CB30FS, UK

*Corresponding author.

Email: mc209@cam.ac.uk (Manish Chhowalla)

Characterization of Li_xMoS_2

X-ray diffraction (XRD) and Raman data of $1\text{T-Li}_x\text{MoS}_2$ material used for cathodes in Na-S batteries are displayed in Figure S1a and b, showing characteristic peaks of the material as reported previously in our papers including Ref. ¹ The material preparation method used here was the same as in our paper Ref. ¹ Figure S1c shows that the material was tested in a Na-ion system with 1 M Sodium trifluoromethanesulfonate (NaCF_3SO_3) in tetraethylene glycol dimethyl ether (TEGDME) electrolyte, confirming its stability within the Na-S voltage window.

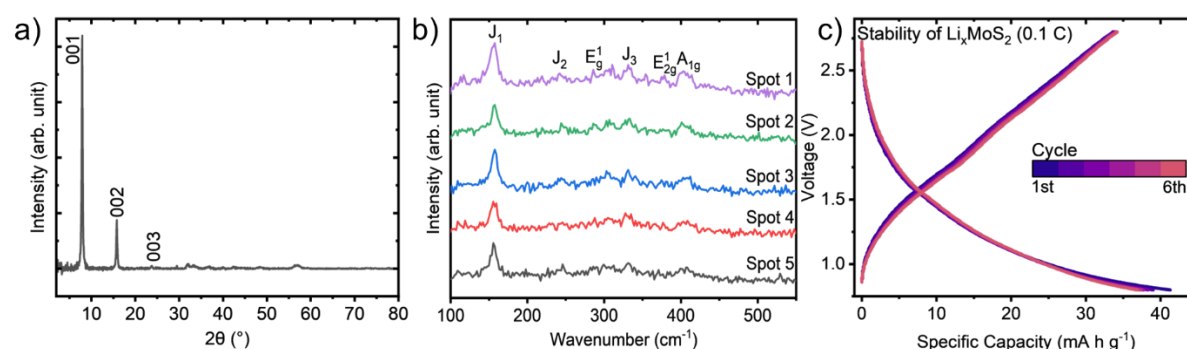


Figure S1. a) X-ray diffraction (XRD) b) Raman spectra of $1\text{T-Li}_x\text{MoS}_2$ at five random locations and c) the cycling of Li_xMoS_2 in Na-ion battery with 1M NaCF_3SO_3 TEGDME electrolyte, showing the reaction region.

Metallic MoS_2 nanosheet hosts for Na-S batteries

We have previously reported that the metallic MoS_2 is a good host for Li-S batteries. ¹ We therefore investigate their viability for the Na-S battery system. The experimental details for coin cell manufacture are described in the Experimental Methods section. We performed galvanic charge-discharge (GCD) measurements on the coin cells at 0.1 C, the 1st cycle of five cells are shown in Figure S2a and the cycling of one battery for 6 cycles is shown in Figure S2b. It can be seen that the coin cell shows capacity fading from 600 mA h g^{-1} to 200 mA h g^{-1} after six cycles. The improved performance in MoS_2 cathode-based battery is due to lower

impedance of the electrodes, shown in Figure S2c, showing that the resistance of the cell increases after 6 cycles. These results indicate that metallic MoS₂ nanosheet-based sulfur hosts show promise for Na-S batteries, demonstrating performance comparable to previous studies.

2-5

Three cyclic voltammetry (CV) scans at 0.1 mV/s scan rate in Figure S2d show that the reduction and oxidation peaks decrease with number of cycles, indicating aging of the battery during discharging and charging and the processes are not reversible due to shuttling of polysulfides. This is also observed in Figure S2e; however, the oxidation peaks reduced from three peaks to two. This may indicate that one of oxidation peaks is not reversible or the higher scan rate does not allow formation of some polysulfides. Finally, the differential capacity curves of the first cycle from Figure S2f, showing that the peaks align with the CV curves.

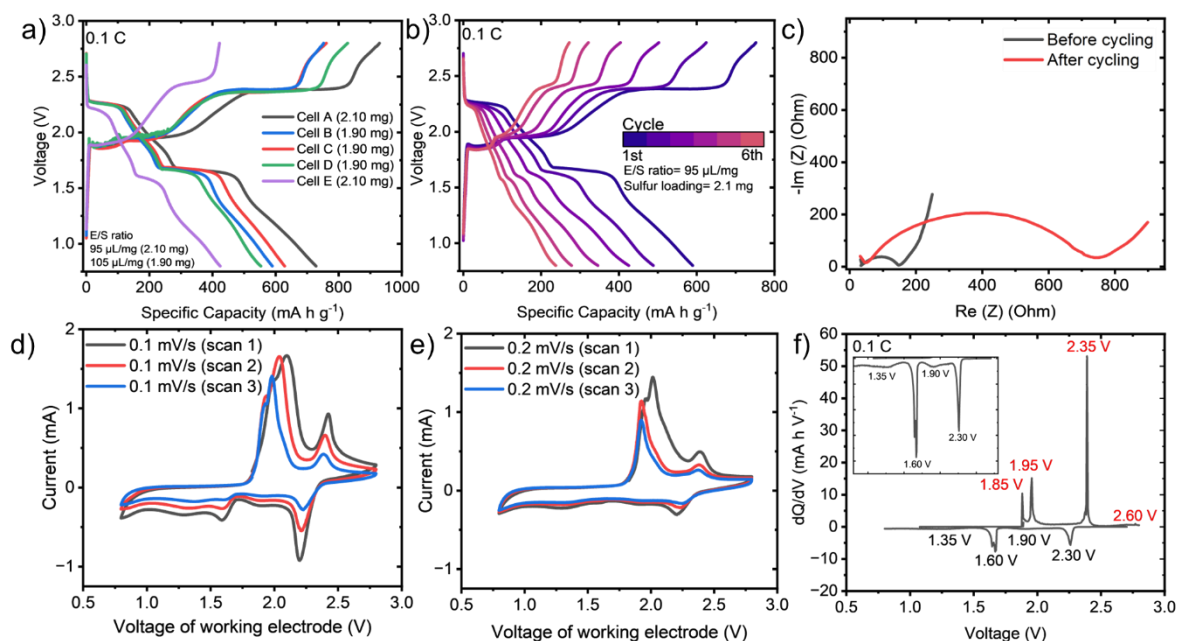


Figure S2. a) Galvanic charge-discharge (GCD) graph first cycle across five cells of the Na-S battery with metallic MoS₂ nanosheets b) Galvanic charge-discharge (GCD) graph of the Na-S battery with metallic MoS₂ nanosheets as the sulfur host, with specific capacity calculated per gram of sulfur. The electrolyte-to-sulfur (E/S) ratio was 95 μ L/mg, and the sulfur loading was 2.1 mg. The capacity fading with cycles is attributed to polysulfide shuttling effects. c)

EIS before and after cycling, showing an increase in resistance. CV of Na-S with 1T-Li_xMoS₂ as the cathode at different scan rates of d) 0.1 mV/s and e) 0.2 mV/s. Three scans for each are shown. At 0.1 mV/s, three peaks are observed, which at 0.2 mV/s, only two oxidation peaks are present. f) The differential capacity curves of the first cycle from Figure S2b.

In depth peak assignments for UV-Vis spectra of molar ratio polysulfide solutions

The UV-Vis spectra displayed in Figure S3 with specific peaks identified in polysulfide solutions with varying molar ratios. These peaks were identified using literature listed in Table S1.

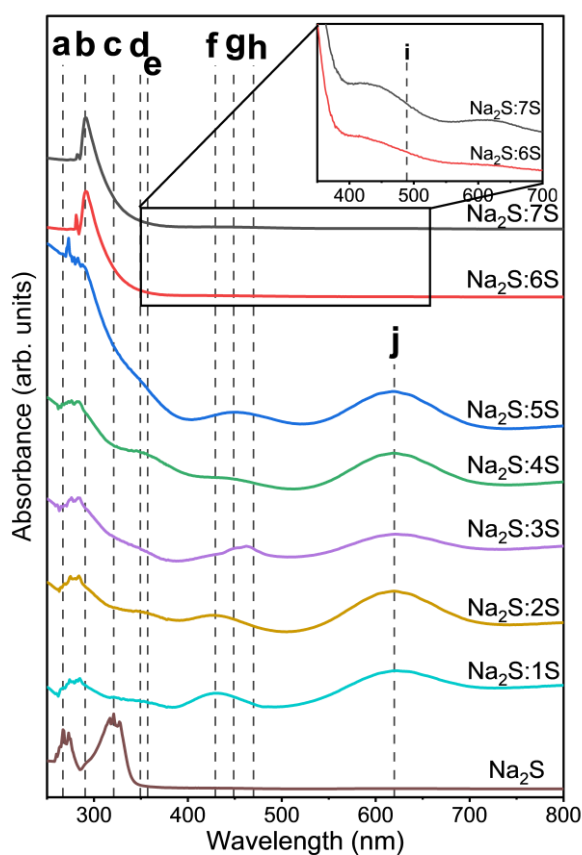


Figure S3. UV-Vis spectra of the reference polysulfide solutions in 1.0 M NaCF₃SO₃ in TEGDME. Significant peaks are labelled a-j, and the responsible species are identified in Table S1.

Table S1. Assignment of polysulfide species peaks from solution of in 1.0 M NaCF₃SO₃ and TEGDME with cross reference values from previous Na-S work, lithium polysulfides and our own research.

Label	Wavelength (nm)	Polysulfide	Reference	Reference reported
a	267	S ²⁻	⁶	250 nm for Li ₂ S in 1 M LiCF ₃ SO ₃ DMF
b	285-290	S ₈ ²⁻ and S ₇ ²⁻	⁷	285 nm for Na ₂ S ₈ , K ₂ S ₈ or Li ₂ S ₈ in THF
c	320	S ²⁻	This work only.	
d	350	S ₆ ²⁻	^{6, 8, 9}	⁶ 340 nm for Li ₂ S ₆ in 1 M LiCF ₃ SO ₃ DMF ⁸ 360 nm for Na ₂ S ₆ in DMF ⁹ 350 nm for for Na ₂ S ₆ in [C ₄ mim][DCA]
e	360	S ₄ ²⁻	^{6, 8}	⁶ 320 and 340 nm for Na ₂ S ₄ in DMF ⁸ 350 nm Na ₂ S ₄ in DMSO
f	430	S ₂ ⁻	^{4, 10, 11}	⁴ 420 nm for Li ₂ S in 1 M LiCF ₃ SO ₃ DMF ¹⁰ S ₂ ⁻ 400 to 450 nm (Li ₂ S ₂ in Hexamethylphosphoramide) ¹¹ 400 nm for S ₂ ⁻ alkali halide single crystals in KCl

g	450	S_4^{2-}	9, 12, 13	<p>⁹ 440 nm for Na_2S_4 in [C₄mim][DCA]</p> <p>¹² Reports a broad peak between 400–500 nm region assigning S_4^{2-} and S_6^{2-} species in 1.5 M $NaClO_4$ and 0.3 M $NaNO_3$ in TEGDME</p> <p>¹³ 435 nm for Na_2S_4 in DMF and DMSO</p>
h	460	S_6^{2-}	6, 8, 9, 12	<p>⁶ 450 nm for Li_2S_6 in 1 M $LiCF_3SO_3$ DMF</p> <p>⁸ 450 nm for Na_2S_6 in DMF</p> <p>⁹ 460 nm for Na_2S_6 in [C₄mim][DCA]</p> <p>¹² Reports a broad peak between 400–500 nm region assigning S_4^{2-} and S_6^{2-} species in 1.5 M $NaClO_4$ and 0.3 M $NaNO_3$ in TEGDME</p>
i	491	S_8^{2-}	6, 14	<p>⁶ 490 nm for Li_2S_8 in 1 M $LiCF_3SO_3$ DMF</p> <p>¹⁴ 492 nm for Na_2S_8 in DMSO</p>
j	620	$S_3^{\cdot-}$	6, 9, 12, 14, 15	<p>⁶ 600 nm for $S_3^{\cdot-}$ species in 1 M $LiCF_3SO_3$ DMF</p>

⁹ 620 nm for S₃^{•-} species in
[C₄mim][DCA]
¹² 620 nm for S₃^{•-} species in
1.5 M NaClO₄ and 0.3 M
NaNO₃ in TEGDME
¹⁴ 618 nm for S₃^{•-} species in
DMSO
¹⁵ 610 nm for S₃^{•-} species in
1 M NaPF₆ Glyme Ether
Solvents

Expanded Raman spectra of sodium polysulfide solutions

The Raman spectra of sodium polysulfide solutions in the 100–1400 cm⁻¹ range, shown in Figure S4, provide an expanded view compared to the spectral range analysed in the main text. This extended wavenumber scale captures peaks up to 1400 cm⁻¹. Notably, beyond 600 cm⁻¹, the spectra primarily reveal peaks associated with electrolyte and S₂O₄²⁻ species, a product of interactions between the solvent and polysulfides. The spectra are annotated to identify the solvent peaks (highlighted in grey) and salt peaks (marked with black dotted lines). The spectra indicate that polysulfide peaks do not occur above 600 cm⁻¹. These peaks were identified using literature listed in Table S2.

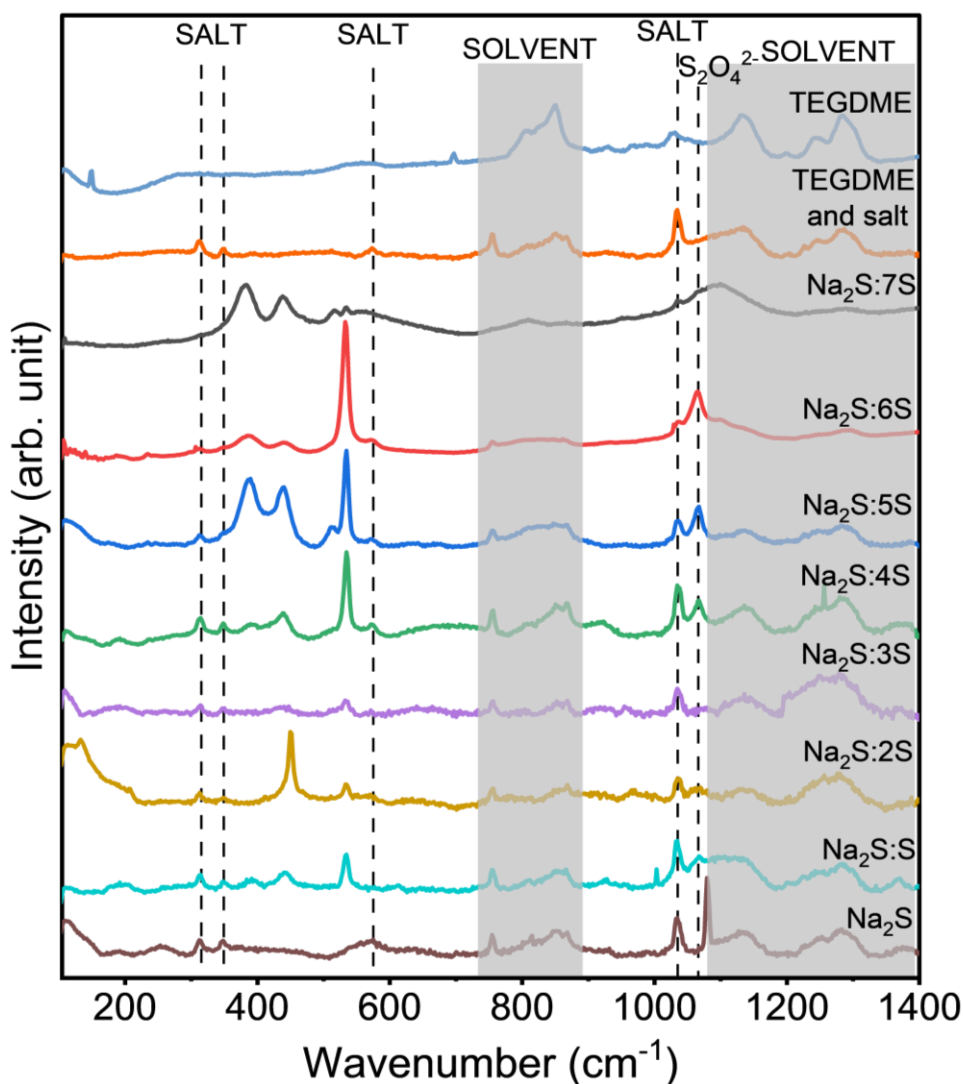


Figure S4. Raman spectra of sodium polysulfide solutions in the 100–1400 cm^{-1} range of the sodium polysulfide solutions. Solvent and salt peaks are labelled.

Table S2. Polysulfide species observed in this work with solutions of 1.0 M NaCF_3SO_3 and TEGDME. Comparison with literature is provided.

Polysulfide (symbol)	Wavenumber (cm^{-1})	Relevant literature	Reference reported
S^{2-} (∇)	119	16	16 reported the 115 cm^{-1} Na-S stretching mode

S_3^{2-} (\square)	132	17	<p>¹⁷ reported 189 cm^{-1} (Li_2)S_3^{2-} in THF (DFT calculation)</p> <p>Within this experimental work this peak is only observed in the molar solution $Na_2S + 2S$.</p>
S_2^{2-} (\blacktriangle)	192	18	<p>¹⁸ reported 134.5 cm^{-1} for polycrystalline Na_2S_2 assigning as Lib motion of the two S_2^{2-} groups in opposite direction.</p>
S_3^{2-} (\square)	207	17	<p>¹⁷ reported 189 cm^{-1} (Li_2)S_3^{2-} in THF (DFT calculation)</p> <p>Within this experimental work this peak is only observed in the molar solution $Na_2S + 2S$.</p>
S_4^{2-} (Bending mode) (\bullet)	234	18-20	<p>¹⁸ reported 239 cm^{-1} (asymmetric bond) and 206 cm^{-1} (symmetric bond) for polycrystalline Na_2S_4</p>

			<p>¹⁹ reported 234 cm⁻¹ for (Li₂)S₄²⁻ (bending mode) in 1 M LiTFSI and TEGDME</p> <p>²⁰ reported 240-245 cm⁻¹ assigned to (Na₂)S₄²⁻ in amines</p>
S ²⁻ (▽)	255	21, 22	<p>²¹ reported 188 cm⁻¹ and 210 cm⁻¹ as S²⁻. This peak was observed in this experimental work only in the solution Na₂S</p> <p>²² reported 190 cm⁻¹ for (Na₂)S²⁻ in TEGDME</p>
S _{8/7} ²⁻ (★)	380	17, 23	<p>¹⁷ reported a DFT calculation assigning 362 cm⁻¹ for (Li₂)S₈²⁻ in THF</p> <p>²³ reported 390 cm⁻¹ most closely corresponds to (Li₂)S₇²⁻ and S₈²⁻ in 1 M LiTFSI, 0.2 M LiNO₃ DME:DOL (1:1)</p>

S_6^{2-} (○)	386	23, 24	<p>²³ reported 365 cm^{-1} corresponds to $(Li_2)S_6^{2-}$ in 1 M LiTFSI, 0.2 M $LiNO_3$ DME:DOL (1:1).</p> <p>²⁴ reported K_2S_6 (S_6^{2-} stretching) at 373 cm^{-1}</p>
S_4^{2-} (●)	390	20, 22, 25	<p>²⁰ reported 393-400 cm^{-1} assigned to $(Na_2)S_4^{2-}$ in amines</p> <p>²² reported 375 cm^{-1} to $(Na_2)S_4^{2-}$ in TEGDME</p> <p>²⁵ reported 400 cm^{-1} for liquid Na_2S_4</p>
S_8^{2-} (★)	436	17, 20	<p>¹⁷ reported DFT calculation of 427 and 429 cm^{-1} for $(Li_2)S_8^{2-}$ in THF</p> <p>²⁰ reported 414, 424 and 440 cm^{-1} assigned to $(Na_2)S_8^{n-}$ in amines</p>
S_6^{2-} (○)	440	23, 26	<p>²³ reported 437 cm^{-1} $(Li_2)S_6^{2-}$ in 1 M LiTFSI, 0.2 M $LiNO_3$ DME:DOL (1:1).</p> <p>²⁶ reports S_6^{2-} at 453 cm^{-1}</p>

S_3^{2-} (□)	450	23, 25, 26	<p>²³ reported 450 cm^{-1} most closely corresponding to $(Li_2)S_4^{2-}$, S_3^{2-}, and S_4^- in 1 M LiTFSI, 0.2 M LiNO₃ DME:DOL (1:1).</p> <p>²⁵ reported 440 cm^{-1} to 462 cm^{-1} assigned to the S-S-S of $(Na_2)S_3^{2-}$ anions</p> <p>²⁶ reports $(Na_2)S_3^{2-}$ at 458 cm^{-1}</p>
S_4^{2-} (●)	518	19, 22	<p>¹⁹ reported 518 cm^{-1} for S_4^- in 1 M LiTFSI and TEGDME</p> <p>²² reports ~500 cm^{-1} to $(Na_2)S_4^{2-}$ in TEGDME</p>
S_3^{*-} (Symmetric stretching mode) (☆)	534	19, 20, 22, 23, 27-30	<p>¹⁹ reported 534 cm^{-1} for S_3^{*-} (Symmetric stretching mode) in 1 M LiTFSI and TEGDME</p> <p>²⁰ reported 533 to 535 cm^{-1} assigned to $(Na_2)S_3^{*-}$ in amines</p> <p>²² reports 534 cm^{-1} to S_3^{*-} in TEGDME</p>

²³ reported 533
cm⁻¹ corresponding to
(Li₂) S₃²⁻ in 1 M
LiTFSI, 0.2 M LiNO₃
DME:DOL (1:1).
²⁷ reported 535 cm⁻¹ as
(Li₂) S₃²⁻ in ammonia
²⁸ and ³⁰ reported 534
cm⁻¹ for S₃²⁻ in NaCl
²⁹ reported 540 cm⁻¹
for an S–S stretch
of a₁ symmetry of S₃²⁻.

UV-Vis Electrochemical set up

The electrochemical set-up for the *ex-situ* UV-Vis study for NaPS.

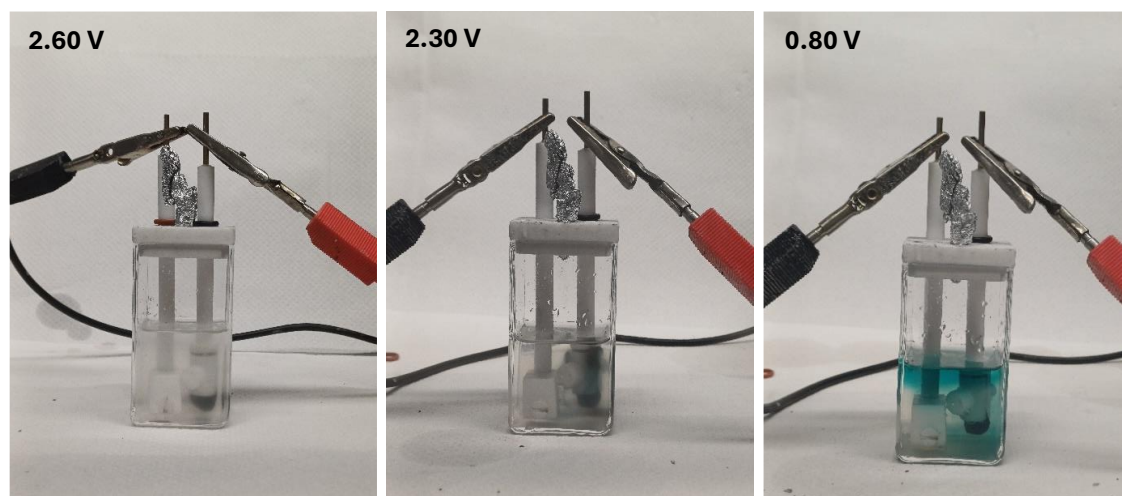


Figure S5. The set up of the electrochemical cell for the *ex-situ* UV-Vis analysis. The photographs are taken at 2.60 V, 2.30 V and 0.8 V (from left to right) during the first discharge in the first cycle.

UV-vis spectra taken on 1st charge and 6th charge for Na-S *ex-situ* is shown in Figure S6. These spectra aimed to reveal how polysulfide species evolve with cycling; however, the data lacked the expected distinction between polysulfide states. This was due to the localized nature of polysulfide conversion, which primarily occurs at the electrode surface, while the aliquots were drawn from bulk electrolyte solutions. As a result, the spectra did not effectively capture minor concentration changes of reaction intermediates, limiting the detection of subtle transformations in these small-volume samples compared to bulk measurements.

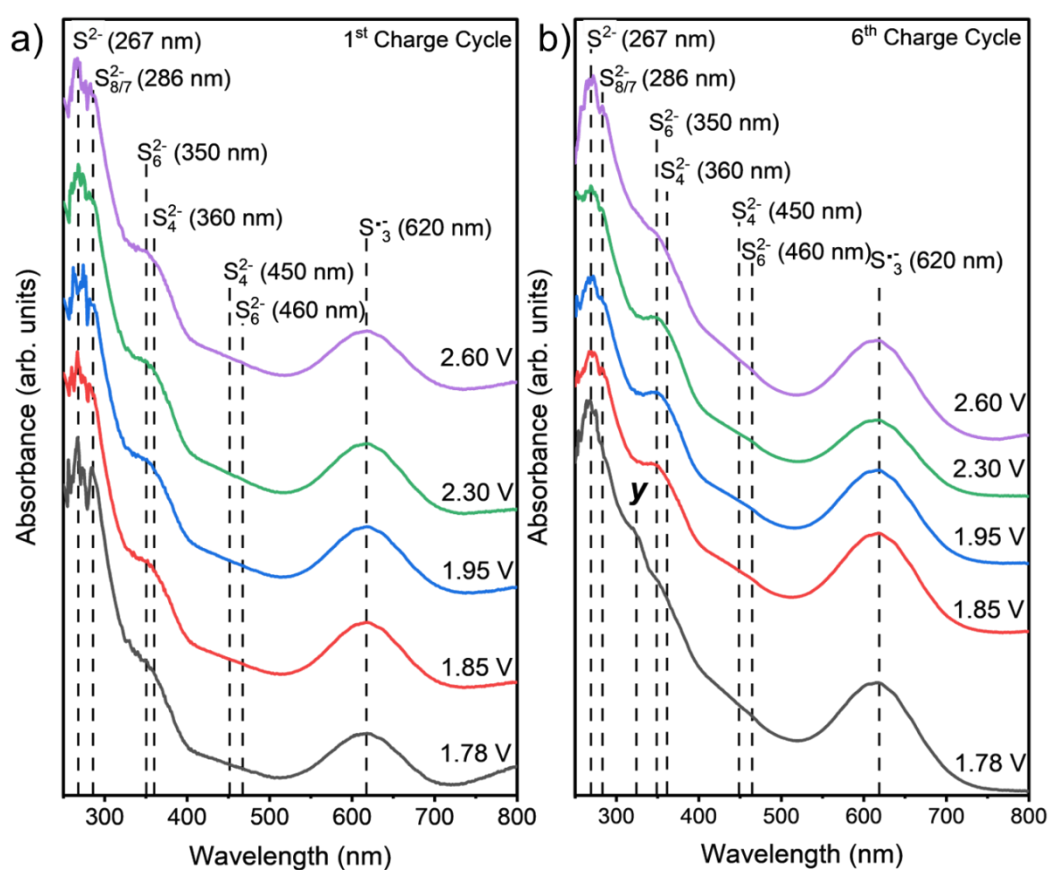


Figure S6. UV-Vis spectra of a) 1st charge b) 6th charge cycle of the Na-S battery.

References

- (1) Li, Z.; Sami, I.; Yang, J.; Li, J.; Kumar, R. V.; Chhowalla, M. Lithiated metallic molybdenum disulfide nanosheets for high-performance lithium–sulfur batteries. *Nature Energy* **2023**.
- (2) Ryu, H.; Kim, T.; Kim, K.; Ahn, J.-H.; Nam, T.; Wang, G.; Ahn, H.-J. Discharge reaction mechanism of room-temperature sodium–sulfur battery with tetra ethylene glycol dimethyl ether liquid electrolyte. *Journal of Power Sources* **2011**, *196* (11), 5186-5190.
- (3) Kim, I.; Park, J. Y.; Kim, C. H.; Park, J. W.; Ahn, J. P.; Ahn, J. H.; Kim, K. W.; Ahn, H. J. A room temperature Na/S battery using a β'' alumina solid electrolyte separator, tetraethylene glycol dimethyl ether electrolyte, and a S/C composite cathode. *Journal of Power Sources* **2016**, *301*, 332-337, Article. DOI: 10.1016/j.jpowsour.2015.09.120 Scopus.
- (4) Kohl, M.; Borrmann, F.; Althues, H.; Kaskel, S. Hard Carbon Anodes and Novel Electrolytes for Long-Cycle-Life Room Temperature Sodium-Sulfur Full Cell Batteries. *Advanced Energy Materials* **2016**, *6* (6), 1502185. DOI: <https://doi.org/10.1002/aenm.201502185> (accessed 2025/01/24).
- (5) Kim, I.; Park, J.-Y.; Kim, C.; Park, J.-W.; Ahn, J.-P.; Ahn, J.-H.; Kim, K.-W.; Ahn, H.-J. Sodium polysulfides during charge/discharge of the room-temperature Na/S battery using TEGDME electrolyte. *Journal of The Electrochemical Society* **2016**, *163* (5), A611.
- (6) Han, D.-H.; Kim, B.-S.; Choi, S.-J.; Jung, Y.; Kwak, J.; Park, S.-M. Time-Resolved In Situ Spectroelectrochemical Study on Reduction of Sulfur in N, N' -Dimethylformamide. *Journal of The Electrochemical Society* **2004**, *151* (9), E283.
- (7) Tobishima, S.-I.; Yamamoto, H.; Matsuda, M. Study on the reduction species of sulfur by alkali metals in nonaqueous solvents. *Electrochimica Acta* **1997**, *42* (6), 1019-1029.

- (8) Kim, B. S.; Park, S. M. In Situ Spectroelectrochemical Studies on the Reduction of Sulfur in Dimethyl Sulfoxide Solutions. *Journal of The Electrochemical Society* **1993**, *140* (1), 115.
- (9) Manan, N. S. A.; Aldous, L.; Alias, Y.; Murray, P.; Yellowlees, L. J.; Lagunas, M. C.; Hardacre, C. Electrochemistry of Sulfur and Polysulfides in Ionic Liquids. *The Journal of Physical Chemistry B* **2011**, *115* (47), 13873-13879.
- (10) Ledé, B.; Demortier, A.; Gobeltz-Hauteœur, N.; Lelieur, J. P.; Picquenard, E.; Duhayon, C. Observation of the ν_3 Raman band of S_3^- inserted into sodalite cages. *Journal of Raman Spectroscopy* **2007**, *38* (11), 1461-1468.
- (11) Holzer, W.; Murphy, W. F.; Bernstein, H. J. Raman spectra of negative molecular ions doped in alkali halide crystals. *Journal of Molecular Spectroscopy*, **1969**, *32*, 13-23.
- (12) Yu, X.; Manthiram, A. Highly Reversible Room-Temperature Sulfur/Long-Chain Sodium Polysulfide Batteries. *The Journal of Physical Chemistry Letters* **2014**, *5* (11), 1943-1947.
- (13) Bonnaterre, R.; Cauquis, G. Spectrophotometric study of the electrochemical reduction of sulphur in organic media. *Journal of the Chemical Society, Chemical Communications* 1972, (5), 293-294.
- (14) Martin, R. P.; Doub, W. H., Jr.; Roberts, J. L., Jr.; Sawyer, D. T. Electrochemical reduction of sulfur in aprotic solvents. *Inorganic Chemistry* 1973, *12* (8), 1921-1925.
- (15) Carter, R.; NewRingeisen, A.; Reed, D.; Atkinson, R. W., III; Mukherjee, P. P.; Love, C. T. Optical Microscopy Reveals the Ambient Sodium–Sulfur Discharge Mechanism. *ACS Sustainable Chemistry & Engineering* **2021**, *9* (1), 92-100.
- (16) Wen, Q.; Wu, Y.; Wang, X.; Zhuang, Z.; Yu, Y. Researches on preparation and properties of sodium polysulphide as gold leaching agent. *Hydrometallurgy* **2017**, *171*, 77-85.

- (17) Hagen, M.; Schiffels, P.; Hammer, M.; Dörfler, S.; Tübke, J.; Hoffmann, M. J.; Althues, H.; Kaskel, S. In-Situ Raman Investigation of Polysulfide Formation in Li-S Cells. *Journal of The Electrochemical Society* **2013**, *160* (8), A1205.
- (18) Janz, G. J.; Downey, J. R.; Roduner, E.; Wasilczyk, G. J.; Coutts, J. W.; Eluard, A. Raman studies of sulfur-containing anions in inorganic polysulfides. Sodium polysulfides. *Inorganic Chemistry* 1976, *15* (8), 1759-1763.
- (19) Wu, H.-L.; Huff, L. A.; Gewirth, A. A. In Situ Raman Spectroscopy of Sulfur Speciation in Lithium–Sulfur Batteries. *ACS Applied Materials & Interfaces* **2015**, *7* (3), 1709-1719.
- (20) Daly, F. P.; Brown, C. W. Raman spectra of sodium tetrasulfide in primary amines. Evidence for sulfide (S₄²⁻-and S₈ⁿ⁻) ions in rhombic sulfur-amine solutions. *The Journal of Physical Chemistry* **1975**, *79* (4), 350-354.
- (21) Wang, Y.; Luo, Z.; Liu, D.; Li, Y. Immobilization of mercury in tailings originating from the historical artisanal and small-scale gold mining using sodium polysulfide. *Environmental Science and Pollution Research* **2022**, *29*, 1-17.
- (22) Kandhasamy, S.; Nikiforidis, G.; Jongerden, G.; Jongerden, F.; Sanden, M. C. M.; Tsampas, M. Operational strategies to improve the performance and long-term cyclability of intermediate temperature sodium-sulfur (IT-NaS) battery. *ChemElectroChem* 2021, *8*.
- (23) McBrayer, J. D.; Beechem, T. E.; Perdue, B. R.; Apblett, C. A.; Garzon, F. H. Polysulfide Speciation in the Bulk Electrolyte of a Lithium Sulfur Battery. *Journal of The Electrochemical Society* **2018**, *165* (5), A876.
- (24) Janz, G. J.; Coutts, J. W.; Downey, J. R.; Roduner, E. Raman studies of sulfur-containing anions in inorganic polysulfides. Potassium polysulfides. *Inorganic Chemistry* **1976**, *15* (8), 1755-1759.
- (25) El Jaroudi, O.; Picquenard, E.; Gobeltz, N.; Demortier, A.; Corset, J. Raman Spectroscopy Study of the Reaction between Sodium Sulfide or Disulfide and Sulfur:

- Identity of the Species Formed in Solid and Liquid Phases. *Inorganic Chemistry* **1999**, 38 (12), 2917-2923.
- (26) Chivers, T.; Lau, C. Raman spectroscopic identification of the S₄N⁻- and S₃⁻-ions in blue solutions of sulfur in liquid ammonia. *Inorganic Chemistry* **1982**, 21 (1), 453-455.
- (27) Dubois, P.; Lelieur, J. P.; Lepoutre, G. Identification and characterization of lithium polysulfides in solution in liquid ammonia. *Inorganic Chemistry* **1988**, 27 (1), 73-80.
- (28) Chivers, T. Ubiquitous trisulphur radical ion S₃^{-·}. *Nature* **1974**, 252 (5478), 32-33.
- (29) Chivers, T.; Elder, P. J. W. Ubiquitous trisulfur radical anion: fundamentals and applications in materials science, electrochemistry, analytical chemistry and geochemistry. *Chemical Society Reviews* **2013**, 42 (14), 5996-6005.
- (30) Holzer, W.; Murphy, W. F.; Bernstein, H. J. Resonance raman effect of S₃⁻ doped in a NaCl single crystal. *Chemical Physics Letters* **1970**, 4 (10), 641-642.